Publ. Astron. Soc. Japan 38, 285–294 (1986)

Detection of an Intense Iron Line at 6.4 keV in the X-Ray Spectrum of NGC 4151

Masaru MATSUOKA, Takeshi IKEGAMI, Hajime INOUE, and Katsuji KOYAMA

Institute of Space and Astronautical Science, 6-1, Komaba 4-chome, Meguro-ku, Tokyo 153

(Received 1985 September 9; accepted 1986 January 7)

Abstract

The Seyfert galaxy NGC 4151 was observed in January and March, 1984 with the gas scintillation proportional counters on board Tenma. The X-ray intensities for both periods were $(2\text{–}3)\times10^{-3}$ times the Crab Nebula intensity in the 2–10-keV band, the lowest level so far observed. The X-ray spectra reveal intense iron line emission at 6.39 ± 0.07 keV (corrected for the recessional velocity of NGC 4151) with an equivalent width of 318 ± 75 eV (averaged over the two periods). The line center energy indicates that the emission line comes from iron atoms in ionized states lower than Fe XIX, and is most probably due to fluorescence of cool matter illuminated by the continuum X-rays. However, the line flux is too intense to be interpreted by a simple model in which isotropic continuum X-rays from the central source illuminate a uniform sphere of the surrounding matter with the solar abundance of iron.

Key words: Seyfert galaxies; X-ray sources; X-ray spectra.

1. Introduction

The Seyfert galaxy NGC 4151 is one of the nearest and most extensively studied of all active galactic nuclei. The radiation observed at wavelengths from radio to γ-rays is variable on numerous time scales. The emission mechanism and the structure of the emission region in the central active nucleus are still unclarified.

Significant evidence of an iron emission line and/or an iron absorption edge around 6–7 keV has been obtained from Ariel V (Barr et al. 1977), OSO 8 (Mushotzky et al. 1978), and HEAO 1 (Holt et al. 1980). As Holt et al. (1980) pointed out, the strength of the fluorescent iron line relative to the depth of the iron absorption edge is a good measure of physical properties in the X-ray absorbing region surrounding the continuum X-ray source. However, the energy resolution of past observations has been insufficient to resolve spectral features precisely.

In this paper, we present the X-ray spectrum of NGC 4151 observed with the gas scintillation proportional counters (GSPC) on board Tenma. The energy resolution of the GSPC is twice that of the proportional counters used in the past observations,

which enables us to obtain detailed properties of the iron emission line from NGC 4151. In fact the GSPC detected a clear emission line at 6.4 keV from NGC 4151 in spite of the low X-ray intensity level of the source. Indeed the source flux was the lowest observed to date. In this paper we examine the intense iron emission line. To this end we evaluate the iron column density from the depth of the iron K-edge absorption and compare this to the hydrogen column density derived from the low energy cutoff. We then discuss the abundance of iron and the geometrical configuration of the matter responsible for the iron line in relation to the derived column densities. We also discuss the possible existence of some unobserved continuum X-rays to explain the intense iron line emission.

2. Observations and Results

NGC 4151 was observed on two occasions, January 11–15 and March 12–15, 1984 with the GSPC on board Tenma. The performance and characteristics of the GSPC on Tenma have been reported elsewhere (Tanaka et al. 1984; Koyama et al. 1984). The detectors consist of two groups of counters with different hexagonal fields of view, i.e., FWHM of 3°.1 (A-group) and 2°.5 (B-group). The effective areas of the A and B groups during the observations were 320 cm^2 and 240 cm^2, respectively, where one module of the B-group was switched off, because it experienced a gain change. We analyzed the data from each group separately, and since the results obtained were consistent with each other, we combined the data into one set. Total exposure times with useful data on NGC 4151 were 1.9×10^4 s and 2.1×10^4 s for January and March, respec ively. The off-source background data were intermittently obtained in a sky region adjacent to NGC 4151 with a total exposure time of about 5×10^4 s.

The X-ray light curve for these observations is shown in figure 1. Each data point represents the average X-ray flux in the 2–10-keV energy range during a 30–40-min interval after the background subtraction and aspect correction. The X-ray flux changed significantly on a time scale of hours, ranging from 2 to 3 μJy or $(2\text{–}3)\times10^{-3}$ times that of the Crab Nebula in the 2–10-keV range.

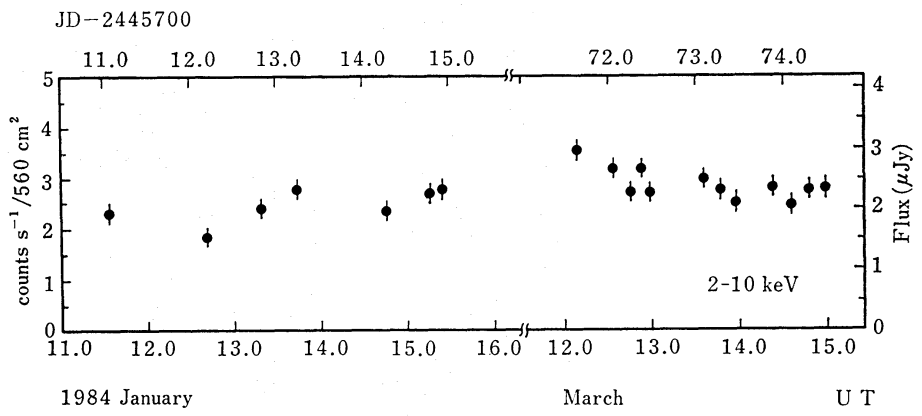

Fig. 1. The X-ray intensity of NGC 4151 as a function of time. The data are typically binned in 30–40-min intervals.

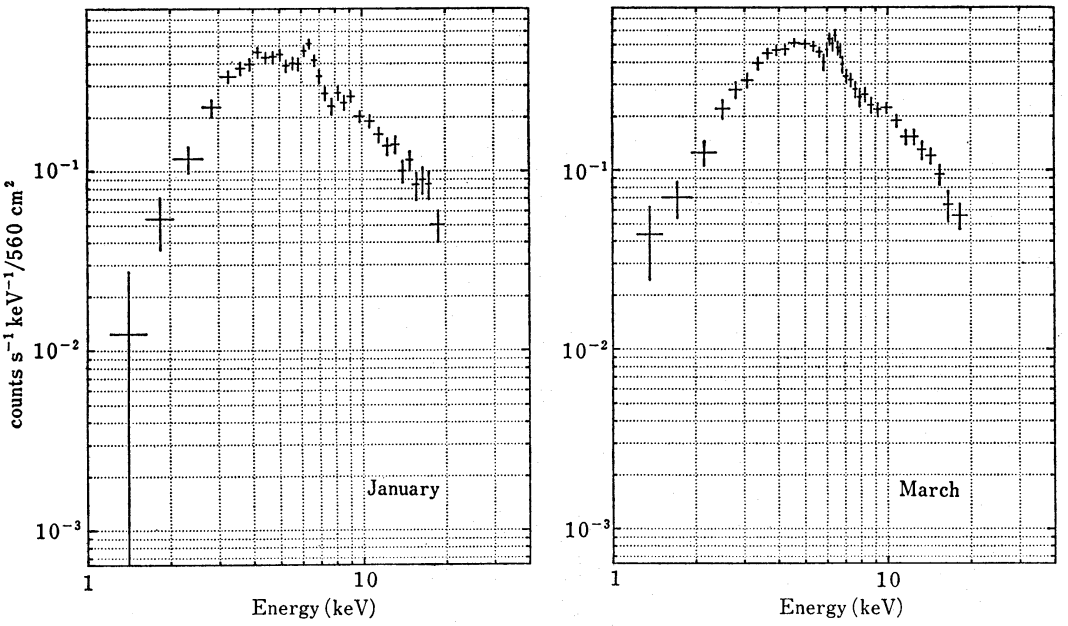

(a)

Fig. 2a. Pulse-height spectra of NGC 4151 without correction for detector response observed in January and March 1984.

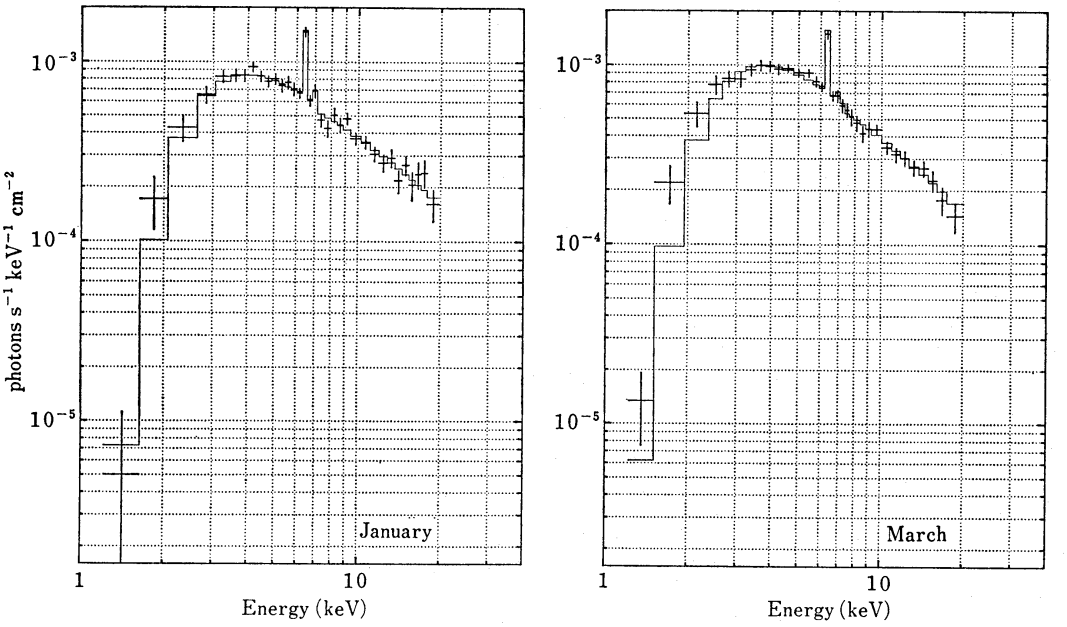

(b)

Fig. 2b. Deconvolved photon spectra of NGC 4151. Solid lines indicate the best-fit power-law spectra with absorption (see table 1 for spectral parameters). The width of the two lines (iron Kα and Kβ) was assumed to be 0.28 keV.

The pulse-height spectra accumulated over each observing period, without correction for detector response, are plotted in figure 2a. The spectra (2–20 keV) are well fitted by a model consisting of a power-law spectrum and an emission line, including photoelectric absorption by neutral matter. The absorption generally takes

Table 1. Typical parameter values in the X-ray band of NGC 4151.

Parameter	Unit	January 11–15, 1984	March 12–15, 1984
α[a]		1.34 ± 0.11	1.44 ± 0.09
A[a]	E^{α}·photons cm^{-2} s^{-1} keV^{-1}	$(0.90\pm0.22)\times10^{-2}$	$(1.12\pm0.25)\times10^{-2}$
I_L[a,b]	photons cm^{-2} s^{-1}	$(2.36\pm0.56)\times10^{-4}$	$(2.51\pm0.49)\times10^{-4}$
E_L[a,c]	keV	6.376 ± 0.081	6.352 ± 0.077
N_H[a]	cm^{-2}	$(7.59\pm0.82)\times10^{22}$	$(6.82\pm0.63)\times10^{22}$
$\chi^2/35$		0.70	0.96
Equivalent width[a,d]	eV	320 ± 75	316 ± 70
Flux (2–10 keV)	$\int F_0$ erg cm^{-2} s^{-1}	$(6.63\pm0.30)\times10^{-11}$	$(6.91\pm0.27)\times10^{-11}$
	$\int F_0 e^{-\sigma N_H}$ erg cm^{-2} s^{-1}	$(2.81\pm0.13)\times10^{-11}$	$(3.19\pm0.12)\times10^{-11}$

[a] Errors represent the 90% confidence level for a single parameter obtained by adjusting parameters, α, A, I_L, E_L, and N_H.

[b] Apparent flux without correction for absorption.

[c] Apparent energy without correction for the recessional velocity of NGC 4151.

[d] Defined as the ratio of the observed line flux to the observed continuum flux at the derived line energy.

For reference the best-fit spectrum obtained from HEAO-1 data on 1978 June 16 and 18 is $0.05E^{-1.55}$ exp $(-5.8\times10^{22}\sigma)$ photons cm^{-2} s^{-1} keV^{-1} (Holt et al. 1980).

the form of an iron K-absorption edge as well as a low-energy cutoff. The energy of the emission line is in the range 6–7 keV. Table 1 summarizes the best-fit values and uncertainty ranges for five free parameters given by a model of the form $[AE^{-\alpha}+I_L(E_L)g(E_L, \Delta)]\exp(-\sigma N_H)$, where the parameters are normalization factor A and spectral index σ of a power-law continuum spectrum, energy E_L and intensity I_L of the emission line, and hydrogen column density N_H of an X-ray absorber. We also present the reduced χ^2 values. A Gaussian distribution is assumed for the function $g(E, \Delta)$ concerning the line, where the width Δ is fixed to be small in comparison to the energy resolution of the GSPC. The quoted errors denote the 90% confidence level for a single parameter. In our estimation of the hydrogen column density, we have assumed cosmic abundances for the neutral elements (e.g., Allen 1973) responsible for the X-ray absorption. The integrated X-ray fluxes over the range 2–10 keV in table 1 are evaluated from the best-fit model spectra. Notice that the X-ray flux in March is slightly larger than that in January as seen in figure 1 and table 1, although the nonabsorbed fluxes are not significantly different from each other. However, no significant change in the values of A, α, and N_H was found for the two spectra. Correlations between these parameters in the spectral fitting make it unclear which parameter causes the change in the flux. On the other hand, it should be noted that the energy of the emission line is determined independently of the other parameters.

The fluxes and the energy centroids of the emission lines in the two spectra are the same within the errors. The equivalent widths of the lines are calculated, and their values also do not differ significantly from each other (see table 1). Taking into account the recession velocity of NGC 4151, 980 km s^{-1} (Anderson and Kraft 1969), the line energy intrinsic to NGC 4151 is estimated to be 6.39 ± 0.07 keV averaged over the two observations. This range includes the Kα-lines of Fe I–Fe XIX [see Mori et al.

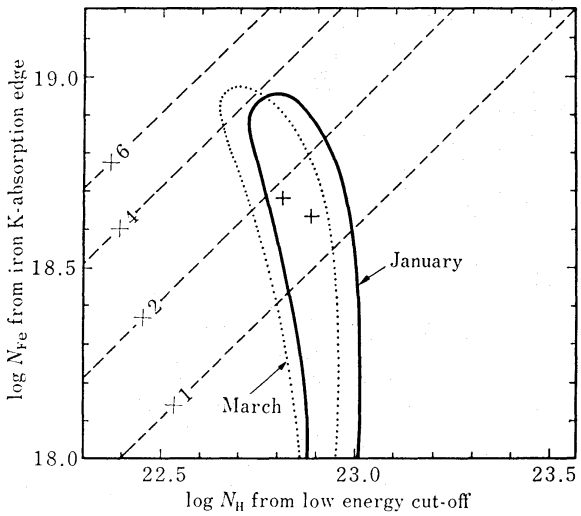

Fig. 3. The 90% confidence contours in the N_{Fe} vs. N_H plane. N_{Fe} and N_H denote the iron column density determined from the iron K-absorption edge and the column density determined by the low-energy absorption, respectively. The chi-square minima are indicated by crosses. The diagonal dashed lines indicate the iron abundance relative to the solar value.

(1979) and Younger (1982) for the energies of K-lines of iron]. The upper limit to the intrinsic line width is evaluated to be about 0.7 keV (FWHM). Deconvolved photon spectra based on the best-fit model are also shown in figure 2b. We took into account an iron Kβ line in the present analysis by fixing the energy and intensity of the Kβ line relative to Kα. However, the effect of the Kβ line on the values of the flux and energy of the Kα line was small, certainly within the statistical uncertainties.

In the above spectral analysis, the abundance of iron relative to that of hydrogen was fixed at the solar value of 4×10^{-5} (e.g., Allen 1973). However, the present spectra allow the column density of iron contributing to the bound-free absorption above the K-edge (>7 keV) to be determined independently of that of the lighter elements responsible for the absorption at lower energies. Therefore, in order to obtain information about the iron abundance, we performed a further spectral fitting to the two spectra in figure 2a, where the iron column density N_{Fe} was introduced as another free parameter in addition to the above five parameters.

The uncertainty ranges on the iron column density obtained from the two spectra are plotted in figure 3 as a function of the hydrogen column density derived from the low-energy cutoff. The solid and dotted curves represent the 90% confidence levels for the two parameters, while the diagonal dashed lines indicate the abundance of iron relative to the solar value. Although the error contours include iron abundance as large as 3.6 and 4.7 times solar, both are also consistent with the solar value. Here, we note that in this analysis the iron line intensity was correlated with the iron column density, but the range of values so derived was consistent with the previous ones (see table 1) over the allowed range of N_{Fe}.

Finally we wish to draw attention to the apparent low-energy deviations from the best-fit spectra in figure 2b. Inspired by the evidence for partial absorption detected with the Solid State Spectrometer (SSS) on board the Einstein Observatory (Holt

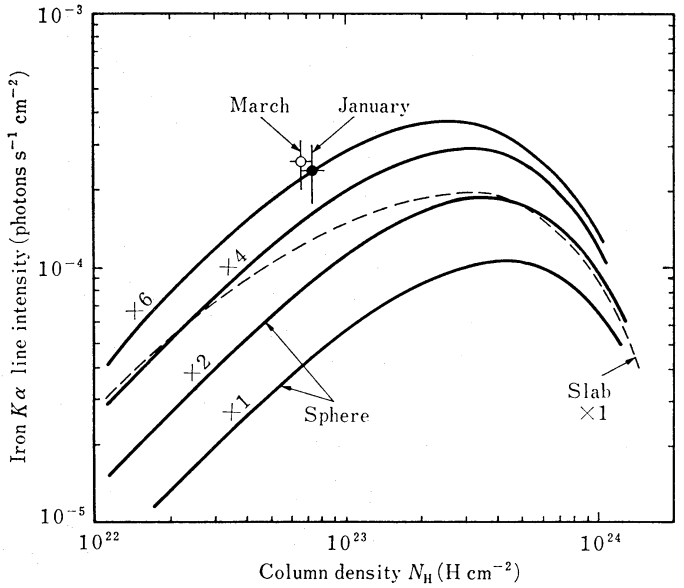

Fig. 4. Comparison of the observed iron intensities at the 90% confidence level with those of various models. Intensities of the iron Kα line were computed by a Monte Carlo simulation assuming that the fluorescence matter has a uniform sphere or slab geometry. The curves are labelled by the abundance of iron relative to the solar value. The incident X-ray spectrum was assumed to be a power law with a normalization factor of $A=1.0\times10^{-2}$ and index $\alpha=1.40$ (average values in table 1).

et al. 1980), we have performed an additional analysis, in which we assumed a power-law spectrum with a leaky absorber. This requires the introduction of one more free parameter, the uncovered fraction of the source. We obtained an upper limit to the uncovered fraction of 15%, consistent with the result of Holt et al. (1980).

3. Discussion

The X-ray flux from NGC 4151 was as weak as a few times 10^{-3} of the Crab Nebula flux in the 2–10-keV range during January and March, 1984. EXOSAT observed this source in December, 1983 and in April, 1984 and the fluxes during these periods were slightly stronger than but comparable to that of the present observation (Pounds et al. 1985, 1986). The present flux level is the lowest reported to date [e.g., Baity et al. (1984) and references therein]. In spite of the low intensity level, we have obtained, for the first time, a detailed measurement of the iron emission line from NGC 4151, using the superior energy resolution and large effective area of the Tenma GSPC. Previous observations of this iron emission line (Barr et al. 1977; Mushotzky et al. 1978; Holt et al. 1980) have not been able to determine its energy and intensity with the precision of the present observation.

The average line energy of 6.39 ± 0.07 keV indicates emission from iron atoms in ionization states lower than Fe XIX. This strongly suggests that the iron line from NGC 4151 is produced by fluorescence of the continuum X-rays acting on cool matter with a temperature lower than 10^7 K (Morita and Fujita 1983), and is not a result of collisional transitions in a hot plasma. The average equivalent width of the line is estimated to be 318 ± 75 eV, consistent with those of past observations (Mushotzky

et al. 1978; Holt et al. 1980). The present continuum is weaker by a factor of about 4 than that observed with HEAO 1 in 1978 (Holt et al. 1980) and the approximate constancy of the equivalent width against a change in the continuum flux is consistent with the fluorescence origin for the line.

We performed a Monte Carlo simulation for the fluorescence of neutral iron atoms distributed spherically about an X-ray source, assumed to radiate isotropically. The fluorescence iron line intensity from the simulations is plotted in figure 4 as a function of the radial column density, $N_{\rm H}$, of a sphere, along with the observed values for NGC 4151. For the incident X-ray spectrum, we employed a power law with a normalization factor of $A=1.0\times10^{-2}$ photons cm^{-2} s^{-1} keV^{-1} and spectral index of $\alpha=1.40$, the values which are consistent with our observed spectra (see table 1). We find that the simulated iron line intensity is proportional to the normalization factor A, but is little affected by the power-law index within the error range. The simulations were also performed by varying the iron abundance and the results for four cases are plotted in figure 4. The fluorescence iron line intensity first increases with the thickness $N_{\rm H}$ of the ambient matter, but when $N_{\rm H}$ becomes larger than $(3\text{–}5)\times10^{23}$ cm^{-2}, the line intensity starts to decrease due to the self-absorption of the photons by the matter.

From figure 4 we see that, under the assumption of spherical symmetry in the X-ray illumination and the spherical and uniform distribution of the fluorescence matter, an overabundance of iron 5–7 times solar is necessary to explain the intense iron line from NGC 4151. Holt et al. (1980) reported a similar overabundance from the optical depth in the iron K-edge of HEAO 1 data at a factor 3.6 ± 1.0. They also proposed an overabundance of $Z\geq14$ elements to explain the 0.6–4-keV spectrum of NGC 4151 observed with the Einstein SSS. However, the present data indicate that the iron column density of the ambient matter derived from the bound-free absorption (at the iron K-edge) sets only an upper limit to the iron abundance of 4–5 times solar (90% confidence level), as seen from figure 3. Therefore, it seems quite likely that an overabundance of iron can only partially explain the intense iron line from NGC 4151, and that it is necessary to introduce some anisotropy in the geometry of the fluorescing matter and/or the continuum X-ray source.

In the above simulations, it was assumed that the observed absorption column density corresponded to the radius of a uniform sphere surrounding the continuum X-ray source. However, the observed absorption column density represents only the matter thickness in the line of sight between the continuum emitter and the observer. Clearly, if the thickness of the surrounding matter were much larger on average than the absorption column density in the line of sight, we could obtain a larger equivalent width for the fluorescence iron line. As seen in figure 4, for example, if the average column density of the sphere were as large as 5×10^{23} cm^{-2} and the matter only in the line of sight happened to have a thickness as small as observed, then the line intensity would be about 2.5 times as large as that from a uniform sphere with a thickness of the observed value ($\sim7\times10^{22}$ cm^{-2}).

As an example of an extreme case for the anisotropy of the ambient matter, we assumed that the continuum X-ray source was embedded in the center of a slab with a half-thickness of $N_{\rm H}$ in the line of sight and an infinite extent in the two other (per-

pendicular) directions. In this case, matter with a thickness much larger than the observed absorption density exists out of the line of sight; furthermore, self absorption of the line photon is less dramatic than in the case of a sphere with a thickness as large as 5×10^{23} cm^{-2}. The resulting iron line intensity for this case is also plotted in figure 4 as a function of $N_{\rm H}$ and the solar abundance of iron. As seen from this figure, the observed iron line intensity is about twice the value expected from a slab with a half-thickness of the observed absorption column density. Therefore, as long as the solar iron abundance is assumed, the anisotropy of the fluorescent matter surrounding the continuum source cannot totally explain the intense iron line emission from NGC 4151 except (possibly) by means of somewhat artificial ad hoc geometries.

The optical broad line region (BLR) is a likely candidate for the source of the 6.4-keV fluorescence iron line (Holt et al. 1980; Ferland and Mushotzky 1982). Considerable research on the nature of the BLR has led to a picture in which the material has a density of 10^{9-10} cm^{-3} and temperature of about 10^4 K in clouds with a typical dimension of the order of 10^{13} cm. Thus the typical column density of each BLR cloud is expected to be 10^{22-23} cm^{-2} [Ferland and Mushotzky (1982) and references therein]. On the other hand, X-ray spectral data from NGC 4151 taken with the Einstein SSS show a soft excess above a uniform absorption model (Holt et al. 1980). As mentioned above Holt et al. (1980) suggested that the SSS data can be explained in terms of a clumped absorber with an approximately 10% uncovered factor. The present spectra and time variation of the absorption column density are also consistent with their picture. Thus, the X-ray absorbing clouds probably correspond to the BLR clouds.

Lawrence and Elvis (1982) studied the correlation between the axial ratio of various Seyfert galaxies and their X-ray and optical/infrared intensities. They suggested that the BLR (or the region immediately surrounding it) has a flattened configuration, parallel to the disk of the parent galaxy. Since NGC 4151 is a typical face-on galaxy (Davies 1973; Simkin 1975), the flattened configuration of the BLR may be similar to the slablike geometry considered above. If this is generally true, however, a larger absorbing column density than that of NGC 4151 would be expected in the X-ray spectra from edge-on active galaxies with low X-ray luminosity. Although Mushotzky (1982) and Lawrence and Elvis (1982) suggest an anticorrelation between X-ray luminosity and X-ray absorption column density, the absorption column density of NGC 4151 is the highest observed even in the sample of low X-ray luminosity Seyfert galaxies.

On the other hand, as yet there are no observational constraints on the geometry of the continuum X-ray emission from the central engine in NGC 4151. A radio jet is observed in NGC 4151 (Johnston et al. 1982) and many other active galactic nuclei also exhibit radio jets (Bridle and Perley 1984). A recent report of narrow and variable lines in the ultraviolet spectrum of NGC 4151 has also been interpreted in terms of excitation by a two-sided jet (Ulrich et al. 1985), while anisotropic radial motions have been found from observations of the distribution of ionized gas (Ulrich 1973; Fricke and Reinhart 1974). This is perhaps evidence for anisotropic propagation of activity from the central engine. Extended soft X-ray emission from NGC 4151 has been observed with the Einstein High Resolution Imager (Elvis et al. 1983), and although the radio jet is at a different position angle from this X-ray emission,

this emission may also reflect anisotropic activity in the X-ray band. Again, observations of X-ray jets in Vir A (Schreier et al. 1982) and Cen A (Feigelson et al. 1981) clearly demonstrate the jetlike activity at X-ray energies for some active galactic nuclei.

Based on the above discussion it appears plausible that some anisotropy might exist in the energy flow from the central engine in the active galactic nucleus of NGC 4151. If so, the intense iron line from NGC 4151 may be interpreted in terms of an intense X-ray beam out of the line of sight. These unobservable X-rays must correspond to a luminosity several times larger than that calculated from the observed continuum flux, if the iron abundance is solar and the ambient fluorescence matter is isotropic. Although this possibility is very attractive in relation to the acceleration mechanism of the jet, we have no other observational evidence at present to support the presence of anisotropy in the continuum X-ray emission from NGC 4151.

The geometrical configuration of the BLR matter and the radiation pattern of the continuum emission from the central engine in the active galactic nuclei still need future study. It is vital to increase the sample of low-luminosity Seyfert galaxies for which X-ray spectra, and in particular the properties of the iron emission line and absorption features, have been investigated in detail. This information will yield important clues for resolving some of the crucial problems in the study of active galactic nuclei such as the origin of the enormous energy output and the mechanism of jet acceleration.

Note added in proof: One more possibility to explain the observed intense iron line from NGC 4151 is proposed as follows: If the fluorescence matter is located further away from a compact X-ray emitting region, the fluorescence iron line emission would be delayed in comparison to the direct continuum X-rays. This suggests that the iron line intensity does not necessitate correlating to the simultaneous continuum intensity. Further long-term observations are necessary to check this possibility.

We would like to thank the Tenma team for providing the present data. Many thanks for a critical reading of the manuscript and for valuable comments are due to Professors S. Hayakawa and K. A. Pounds. We are also grateful to Drs. J. P. Hughes and F. Nagase for their comments.

References

Allen, C. W. 1973, *Astrophysical Quantities*, 3d ed. (Athlone Press, London), p. 31.
Anderson, K. S., and Kraft, R. P. 1969, *Astrophys. J.*, **158**, 859.
Baity, W. A., Mushotzky, R. F., Worrall, D. M., Rothschild, R. E., Tennant, A. F., and Primini, F. A. 1984, *Astrophys. J.*, **279**, 555.
Barr, P., White, N. E., Sanford, P. W., and Ives, J. C. 1977, *Monthly Notices Roy. Astron. Soc.*, **181**, 43P.
Bridle, A. H., and Perley, R. A. 1984, *Ann. Rev. Astron. Astrophys.*, **22**, 319.
Davies, R. D. 1973, *Monthly Notices Roy. Astron. Soc.*, **161**, 25P.
Elvis, M., Briel, U. G., and Henry, J. P. 1983, *Astrophys. J.*, **268**, 105.
Feigelson, E. D., Schreier, E. J., Delvaille, J. P., Giacconi, R., Grindlay, J. E., and Lightman, A. P. 1981, *Astrophys. J.*, **251**, 31.

Ferland, G. J., and Mushotzky, R. F. 1982, *Astrophys. J.*, **262**, 564.
Fricke, K. J., and Reinhardt, M. 1974, *Astron. Astrophys.*, **37**, 349.
Holt, S. S., Mushotzky, R. F., Becker, R. H., Boldt, E. A., Serlemitsos, P. J., Szymkowiak, A. E., and White, N. E. 1980, *Astrophys. J. Letters*, **241**, L13.
Johnston, K. J., Elvis, M., Kjer, D., and Shen, B. S. P. 1982, *Astrophys. J.*, **262**, 61.
Koyama, K., Ikegami, T., Inoue, H., Kawai, N., Makishima, K., Matsuoka, M., Mitsuda, K., Murakami, T., Ogawara, Y., Ohashi, T., Suzuki, K., Tanaka, Y., Waki, I., and Fenimore, E. E. 1984, *Publ. Astron. Soc. Japan*, **36**, 659.
Lawrence, A., and Elvis, M. 1982, *Astrophys. J.*, **256**, 410.
Mori, K., Otsuka, M., and Kato, T. 1979, *Atom. Data Nucl. Data Tables*, **23**, 195.
Morita, S., and Fujita, J. 1983, *J. Phys. Soc. Japan*, **52**, 1957.
Mushotzky, R. F. 1982, *Astrophys. J.*, **256**, 92.
Mushotzky, R. F., Holt, S. S., and Serlemitsos, P. J. 1978, *Astrophys. J. Letters*, **225**, L115.
Pounds, K. A., Warwick, R. S., Culhane, J. L., and de Korte, P. 1985, *Space Sci. Rev.*, **40**, 585.
Pounds, K. A., Warwick, R. S., Culhane, J. L., and de Korte, P. A. J. 1986, *Monthly Notices Roy. Astron. Soc.*, **218**, 685.
Schreier, E. J., Gorenstein, P., and Feigelson, E. D. 1982, *Astrophys. J.*, **261**, 42.
Simkin, S. M. 1975, *Astrophys. J.* **200**, 567.
Tanaka, Y., Fujii, M., Inoue, H., Kawai, N., Koyama, K., Maejima, Y., Makino, F., Makishima, K., Matsuoka, M., Mitsuda, K., Murakami, T., Nishimura, J., Oda, M., Ogawara, Y., Ohashi, T., Shibazaki, N., Suzuki, K., Waki, I., Yamagami, T., Kondo, I., Murakami, H., Hayakawa, S., Hirano, T., Kunieda, H., Masai, K., Nagase, F., Sato, N., Tawara, Y., Kitamoto, S., Miyamoto, S., Tsunemi, H., Yamashita, K., and Nakagawa, M. 1984, *Publ. Astron. Soc. Japan*, **36**, 641.
Ulrich, M.-H. 1973, *Astrophys. J.*, **181**, 51.
Ulrich, M. H., Altamore, A., Boksenberg, A., Bromage, G. E., Clavel, J., Elvius, A., Penston, M. V., Perola, G. C., and Snijders, M. A. J. 1985, *Nature*, **313**, 747.
Younger, S. M. 1982, *J. Quant. Spectrosc. Radiat. Transfer*, **27**, 541.